Structural Eng. / Earthquake Eng. Vol. 4. No. 1, 73 s-83 s. April 1987
Japan Society of Civil Engineers (Proc. of JSCE No. 380/I-7)

PRINCIPLE AND NUMERICAL CHECK OF A STIFFNESS EQUATION FOR PLANE FRAMES

By Tetsuo IWAKUMA, Akio HASEGAWA**, Fumio NISHINO*** and Shigeru KURANISHI*****

A stiffness equation of plane frames is formulated in finite displacements by the total Lagrangian approach. The formulation is based on the physical interpretation of the polar decomposition theorem and does not use any variational principle. The corresponding differential equations are also given to show which theoretical solutions the discretized ones converge to. For the Bernoulli-Euler beam, the postbuckling behavior can be analysed accurately without the geometric stiffness matrix which helps to accelerate the convergence of solutions. On the other hand, the Timoshenko beam element must have the geometric stiffness in order to obtain the correct solutions. Finally the typical stability problems which have the bifurcation points in their equilibrium paths are solved to demonstrate the ability of the stiffness equation.

Keywords: *total Lagrangian, FEM, Timoshenko beam, finite displacement*

1. INTRODUCTION

In the formulation of stiffness equations in finite displacements, the best and well-established method is to decompose total deformation into finite rotation and infinitesimal deformation, as long as the strains are very small. There are two approaches, one of which is the incremental scheme[1)~3)]. In this approach, the small incremental deformation is superposed on the deformation in the nearest current configuration to derive the tangent stiffness equation. The obtained tangent stiffness equation is nonlinear with respect to the incremental quantities such as incremental displacements.

Another approach is the total Lagrangian scheme[4)~6)] which separates the total deformation into its representative rotation and the real deformation component. In plane problems, the finite rotation can be easily handled, while there may exist some difficulty in dealing with the finite rotation in three dimensions[7)]. Although the stiffness equation has not been explicitly derived in Ref. 5), the accuracy and convergence of this method to describe the governing differential equation of a beam have been already checked. In Ref. 6), the beam-column equation is analytically solved to derive the tangent stiffness matrix, but the conventional stiffness matrices for a beam are not used explicitly. The stiffness equation is nonlinear with respect to the total displacements. Hence becomes necessary to use some iterative scheme to solve it.

We here present the principle on which the derivation of the stiffness equation is based in the total Lagrangian approach, and show the explicit forms of the stiffness equation and its tangent stiffness matrix

* Member of JSCE, Ph. D., Associate Professor, Department of Civil Engineering, Tohoku University (Aoba, Sendai 980)
** Member of JSCE, Dr. Eng., Associate Professor, Division of Structural Engineering and Construction, Asian Institute of Technology (G. P. O. Box 2754, Bangkok 10501, Thailand), on leave from University of Tokyo (Bunkyo-ku, Tokyo 113)
*** Member of JSCE, Ph. D., Professor, Department of Civil Engineering, University of Tokyo
**** Member of JSCE, Dr. Eng., Professor, Department of Civil Engineering, Tohoku University

which are expressed by the commonly used stiffness matrices for a beam in either infinitesimal or linearized finite (relatively small) displacement theory. The convergence of discretized solutions to the elliptic-integral solutions of an elastica and its speed are examined in conjunction with the geometric stiffness matrix for the Bernoulli-Euler beam. The discretized solutions of the Timoshenko beam elements are compared with the numerical-integral solutions of various versions of the governing differential equations, in order to examine their mutual correspondence and also show the important role which the geometric stiffness matrix plays. To obtain the corresponding differential equation is important to judge whether the discretized equation represents a correct physical model or not. Finally, as illustrative examples, some bifurcation problems are analysed without the direct use of the eigenvalue analysis.

2. PRINCIPLE

In the total Lagrangian approach, the formulation of the stiffness equation may be based on the polar decomposition theorem[8] which can be expressed in the matrix form by

$$\boldsymbol{F}\equiv[\partial x_i/\partial X_j]=\boldsymbol{R}\boldsymbol{U},\quad \boldsymbol{R}^{-1}=\boldsymbol{R}^T \cdots\cdots (1)$$

where $\boldsymbol{F}$ is the deformation-gradient tensor; x_i is the i-th component of the current position vector of a particle located initially at $\boldsymbol{X}$, the j-th component of which is denoted by X_j; $\boldsymbol{U}$ is the right stretch tensor which represents the "real" deformation; $\boldsymbol{R}$ is the orthogonal rotation tensor. Namely this theorem simply states that the total deformation is the superposition of the rotation $\boldsymbol{R}$ and the real deformation $\boldsymbol{U}$. While, in the infinitesimal displacement theory, both $\boldsymbol{F}$ itself and $\boldsymbol{U}$ are approximately equal to the identity matrix, only $\boldsymbol{U}$ is approximately the identity matrix in finite displacements, provided that the strain ("real" deformation) is negligibly small.

Utilizing this theorem, we can construct the local stiffness equation symbolically as follows. Consider a small element including one point $\boldsymbol{X}_0$ as a reference point. Then the deformation gradient, $\boldsymbol{F}$, at an arbitrary point in the vicinity of $\boldsymbol{X}_0$ can be approximated by the relative displacements referred to the displacements at $\boldsymbol{X}_0$. Furthermore, if the rotation near the reference point $\boldsymbol{X}_0$ is also represented by the rotation at $\boldsymbol{X}_0$, Eq. (1) results in

$$[\text{Relative Displacements near } \boldsymbol{X}_0]=\boldsymbol{R}(\boldsymbol{X}_0)\,[\text{Real Deformation near } \boldsymbol{X}_0] \cdots\cdots (2)$$

As long as the strains are small, the constitutive relation between the resistance forces of the body and the deformation can be assumed to be linear. Therefore

$$[\text{Resistance Forces near } \boldsymbol{X}_0]=\boldsymbol{K}\,[\text{Real Deformation near } \boldsymbol{X}_0] \cdots\cdots (3)$$

where $\boldsymbol{K}$ is the stiffness coefficient in the infinitesimal or linearized finite displacement theory. Since the constitutive relation, Eq. (3), must hold independently of the finite rotation, $\boldsymbol{R}(\boldsymbol{X}_0)$, the resistance forces in Eq. (3) are related to the stress resultants defined in the spacially fixed coordinate system as

$$[\text{Stress Resultants}]=\boldsymbol{R}(\boldsymbol{X}_0)\,[\text{Resistance Forces}] \cdots\cdots (4)$$

Eliminating the resistance forces and real deformation in Eq. (2), (3) and (4), and using the orthogonality of $\boldsymbol{R}$, we can express the stiffness equation near $\boldsymbol{X}_0$ as

$$[\text{Stress Resultants}]=\boldsymbol{R}(\boldsymbol{X}_0)\boldsymbol{K}\boldsymbol{R}(\boldsymbol{X}_0)^T\,[\text{Relative Displacements}] \cdots\cdots (5)$$

In the next section, this symbolic expression of the stiffness relation can be reduced to the element stiffness equation of a structure.

3. STIFFNESS EQUATION AND TANGENT STIFFNESS

The principle presented above can be easily applied to the finite displacement theory of plane frames. Consider an element of length l in Fig. 1. If the finite rotation of this element is represented by the rotation at point 1, the infinitesimal or linearized finite displacement theory applies to the beam in the ξ-η coordinate system. Therefore Eq. (3) holds in this ξ-η system. Then, according to the relation in Eq. (5), the stiffness equation for one element can be given as

$$\left.\begin{aligned} \boldsymbol{f}_1 &= \boldsymbol{T}(\lambda_1)\boldsymbol{k}_1(\boldsymbol{d}_1, \boldsymbol{d}_2)\boldsymbol{T}(\lambda_1)^T\{\boldsymbol{d}_2-\boldsymbol{d}_1-\boldsymbol{D}(\lambda_1)\} \\ \boldsymbol{f}_2 &= \boldsymbol{T}(\lambda_1)\boldsymbol{k}_2(\boldsymbol{d}_1, \boldsymbol{d}_2)\boldsymbol{T}(\lambda_1)^T\{\boldsymbol{d}_2-\boldsymbol{d}_1-\boldsymbol{D}(\lambda_1)\} \end{aligned}\right\} \cdots\cdots (6)$$

where $\boldsymbol{f}_i$ and $\boldsymbol{d}_i$ $(i=1, 2)$ are the nodal force and displacement vectors at the i-th node defined by

$$\left.\begin{aligned} \boldsymbol{f}_i &\equiv [F_{xi}L^2/EI \quad F_{yi}L^2/EI \quad C_iL/EI]^T \\ \boldsymbol{d}_i &\equiv [u_i/L \quad v_i/L \quad \lambda_i]^T \end{aligned}\right\} \cdots\cdots (7)$$

where F_{xi}, F_{yi} and C_i are the x- and y-components of nodal force and the applied moment about z-axis at the i-th node, and L denotes the representative length of the structure which is introduced for non-dimensionalization. $\boldsymbol{T}(\lambda_1)$ expresses the rotation of this element and is identical with the coordinate transformation matrix between the x-y and ξ-η coordinate systems; i. e.

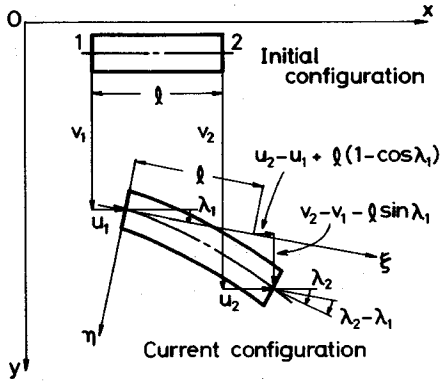

Fig. 1 Relative Displacement Components.

$$\boldsymbol{T}(\lambda_1) \equiv \begin{bmatrix} \cos\lambda_1 & -\sin\lambda_1 & 0 \\ \sin\lambda_1 & \cos\lambda_1 & 0 \\ 0 & 0 & 1 \end{bmatrix} \cdots\cdots (8)$$

$\boldsymbol{D}(\lambda_1)$ is the displacement of node 2 as a rigid body due to the rotation of the element; i. e.

$$\boldsymbol{D}(\lambda_1) \equiv \{(\cos\lambda_1-1)/\zeta \quad (\sin\lambda_1)/\zeta \quad 0\}^T \cdots\cdots (9)$$

where ζ is the ratio of the representative length, L, to the element length defined by

$$\zeta \equiv L/l \cdots\cdots (10)$$

and therefore $(\boldsymbol{d}_2-\boldsymbol{d}_1-\boldsymbol{D}(\lambda_1))$ is the relative displacement vector. Finally $\boldsymbol{k}_1$ and $\boldsymbol{k}_2$ are given by[9]

$$\boldsymbol{k}_i(\boldsymbol{d}_1, \boldsymbol{d}_2) = \boldsymbol{k}_{iL} + z_0(\boldsymbol{d}_1, \boldsymbol{d}_2)\boldsymbol{k}_{iNL} \qquad (i=1, 2)$$

$$\left.\begin{aligned} \boldsymbol{k}_{1L} &\equiv \begin{bmatrix} -\zeta/\beta^2 & 0 & 0 \\ 0 & -12\zeta^3/\Delta_0 & 6\zeta^2/\Delta_0 \\ 0 & -6\zeta^2/\Delta_0 & (2-12\phi)\zeta/\Delta_0 \end{bmatrix}, \quad \boldsymbol{k}_{1NL} \equiv \begin{bmatrix} 0 & 0 & 0 \\ 0 & -6\Delta_1\zeta/(5\Delta_0^2) & 1/(10\Delta_0^2) \\ 0 & -1/(10\Delta_0^2) & (-1/30-\Delta_2)/(\zeta\Delta_0^2) \end{bmatrix} \\ \boldsymbol{k}_{2L} &\equiv \begin{bmatrix} \zeta/\beta^2 & 0 & 0 \\ & 12\zeta^3/\Delta_0 & -6\zeta^2/\Delta_0 \\ \text{Sym.} & & (4+12\phi)\zeta/\Delta_0 \end{bmatrix}, \quad \boldsymbol{k}_{2NL} \equiv \begin{bmatrix} 0 & 0 & 0 \\ & 6\Delta_1\zeta/(5\Delta_0^2) & -1/(10\Delta_0^2) \\ \text{Sym.} & & (2/15+\Delta_2)/(\zeta\Delta_0^2) \end{bmatrix} \end{aligned}\right\} \cdots\cdots (11)$$

where $\boldsymbol{k}_{iL}$ and $\boldsymbol{k}_{iNL}$ are the linear and nonlinear parts of the stiffness matrix, and

$$\left.\begin{aligned} &\beta \equiv \sqrt{I/A}/L, \quad \phi \equiv \alpha\beta^2\zeta^2, \quad \alpha \equiv E/GK, \quad \Delta_0 \equiv 1+12\phi, \quad \Delta_1 \equiv 1+10\Delta_2, \quad \Delta_2 \equiv 2\phi+12\phi^2 \\ &z_0(\boldsymbol{d}_1, \boldsymbol{d}_2) \equiv (\text{Axial Force})L^2/EI = [\{(u_2-u_1)/L-(\cos\lambda_1-1)/\zeta\}\cos\lambda_1 \\ &\qquad +\{(v_2-v_1)/L-(\sin\lambda_1)/\zeta\}\sin\lambda_1]\zeta/\beta^2 \end{aligned}\right\} \cdots\cdots (12)$$

and K is the shear coefficient[10]. Here $\boldsymbol{k}_{iNL}$ can be called the geometric stiffness matrix of the Timoshenko beam, because it corresponds to the conventional geometric stiffness when shear deformation is neglected; i. e. $\alpha=0$.

We employ the Newton-Raphson method to solve the nonlinear discretized equilibrium equation, Eq. (6). Since Eq. (6) is a highly nonlinear equation in terms of the nodal displacements, and is not based on any variational principle, the tangent stiffness matrix becomes very complicated and nonsymmetric. After expanding the right-hand side of Eq. (6) by the Taylor series with respect to the incremental displacements, taking only the first order terms of the small increments of nodal displacements, we can obtain the tangent stiffness equation as

$$\Delta\boldsymbol{f} = \boldsymbol{k}_t(\boldsymbol{d}_1, \boldsymbol{d}_2)\Delta\boldsymbol{d} \cdots\cdots (13)$$

where Δ signifies the small increments, and

$$\Delta\boldsymbol{f} \equiv [\Delta\boldsymbol{f}_1^T \quad \Delta\boldsymbol{f}_2^T]^T, \quad \Delta\boldsymbol{d} \equiv [\Delta\boldsymbol{d}_1^T \quad \Delta\boldsymbol{d}_2^T]^T \cdots\cdots (14)$$

The 6×6 matrix, $\boldsymbol{k}_t$ is the tangent stiffness matrix expressed as

$$\boldsymbol{k}_t \equiv \begin{Bmatrix} \boldsymbol{T}\boldsymbol{k}_1\boldsymbol{T}^T\ (\boldsymbol{d}_2-\boldsymbol{d}_1-\boldsymbol{D}) \\ \boldsymbol{T}\boldsymbol{k}_2\boldsymbol{T}^T\ (\boldsymbol{d}_2-\boldsymbol{d}_1-\boldsymbol{D}) \end{Bmatrix} \begin{Bmatrix} \partial/\partial\boldsymbol{d}_1 \\ \partial/\partial\boldsymbol{d}_2 \end{Bmatrix}^T = \begin{bmatrix} \boldsymbol{H}_{11} & \boldsymbol{H}_{12} & \boldsymbol{H}_{13}+\boldsymbol{S}_1 & \boldsymbol{H}_{14} & \boldsymbol{H}_{15} & \boldsymbol{H}_{16} \\ \boldsymbol{H}_{21} & \boldsymbol{H}_{22} & \boldsymbol{H}_{23}+\boldsymbol{S}_2 & \boldsymbol{H}_{24} & \boldsymbol{H}_{25} & \boldsymbol{H}_{26} \end{bmatrix}$$
$$+ \begin{Bmatrix} \boldsymbol{P}_1 \\ \boldsymbol{P}_2 \end{Bmatrix} [-\cos\lambda_1 \ \ -\sin\lambda_1 \ \ g \ \ \cos\lambda_1 \ \ \sin\lambda_1 \ \ 0] \cdots\cdots (15)$$

where

$$\left.\begin{aligned} &\boldsymbol{H}_i \equiv [\boldsymbol{H}_{i1}\ \boldsymbol{H}_{i2}\ \boldsymbol{H}_{i3}\ \boldsymbol{H}_{i4}\ \boldsymbol{H}_{i5}\ \boldsymbol{H}_{i6}] = \boldsymbol{T}\boldsymbol{k}_i\boldsymbol{T}^T\boldsymbol{C}, \quad \boldsymbol{S}_i \equiv [\boldsymbol{Q}\boldsymbol{k}_i\boldsymbol{T}^T + \boldsymbol{T}\boldsymbol{k}_i\boldsymbol{Q}^T]\{\boldsymbol{d}_2-\boldsymbol{d}_1-\boldsymbol{D}\} \\ &\boldsymbol{P}_i \equiv \zeta\boldsymbol{T}\boldsymbol{k}_{iNL}\boldsymbol{T}^T\{\boldsymbol{d}_2-\boldsymbol{d}_1-\boldsymbol{D}\}/\beta^2 \qquad (i=1,2) \\ &\boldsymbol{C} \equiv \begin{bmatrix} -1 & 0 & (\sin\lambda_1)/\zeta & 1 & 0 & 0 \\ 0 & -1 & -(\cos\lambda_1)/\zeta & 0 & 1 & 0 \\ 0 & 0 & -1 & 0 & 0 & 1 \end{bmatrix}, \quad \boldsymbol{Q} \equiv \begin{bmatrix} -\sin\lambda_1 & -\cos\lambda_1 & 0 \\ \cos\lambda_1 & -\sin\lambda_1 & 0 \\ 0 & 0 & 0 \end{bmatrix} \\ &g \equiv -\{(u_2-u_1)/L-(\cos\lambda_1-1)/\zeta\}\sin\lambda_1+\{(v_2-v_1)/L-(\sin\lambda_1)/\zeta\}\cos\lambda_1 \end{aligned}\right\} \cdots\cdots (16)$$

Employing the Newton-Raphson method to solve Eq. (6) with Eq. (13), we can write the recursive equation to obtain the $(n+1)$th solution as

$$\begin{Bmatrix} \boldsymbol{d}_1 \\ \boldsymbol{d}_2 \end{Bmatrix}^{(n+1)} = \begin{Bmatrix} \boldsymbol{d}_1 \\ \boldsymbol{d}_2 \end{Bmatrix}^{(n)} + \boldsymbol{k}_t(\boldsymbol{d}^{(n)})^{-1} \begin{Bmatrix} \boldsymbol{f}_1-\boldsymbol{T}(\lambda_1^{(n)})\ \boldsymbol{k}_1(\boldsymbol{d}^{(n)})\ \boldsymbol{T}(\lambda_1^{(n)})^T\ \{\boldsymbol{d}_2^{(n)}-\boldsymbol{d}_1^{(n)}-\boldsymbol{D}(\lambda_1^{(n)})\} \\ \boldsymbol{f}_2-\boldsymbol{T}(\lambda_1^{(n)})\ \boldsymbol{k}_2(\boldsymbol{d}^{(n)})\ \boldsymbol{T}(\lambda_1^{(n)})^T\ \{\boldsymbol{d}_2^{(n)}-\boldsymbol{d}_1^{(n)}-\boldsymbol{D}(\lambda_1^{(n)})\} \end{Bmatrix} \cdots\cdots (17)$$

for the displacements at the n-th step known. In the calculations below, the iteration is stopped when $|\boldsymbol{d}^{(n+1)}-\boldsymbol{d}^{(n)}|/|\boldsymbol{d}^{(n+1)}|<10^{-6}$.

It should be noted, however, that all quantities above are defined in the local element coordinate system. In order to construct the global tangent stiffness equation of the plane frame, the commonly used manipulation of the coordinate transformation is needed as is briefly stated below. Suppose that one member is initially inclined by the angle θ from the spacial coordinate system in the same direction of the definition of λ in Fig. 1. If the nodal quantities are also defined in the spacially fixed coordinate system, the tangent stiffness equation (13), for example, must be rewritten as

$$\Delta\boldsymbol{f} = \boldsymbol{T}(\theta)\boldsymbol{k}_t\boldsymbol{T}(\theta)^T\Delta\boldsymbol{d} \cdots\cdots (18)$$

in the spacial reference coordinate system, in which $\boldsymbol{T}$ is defined in Eq. (8). The evaluation of $\boldsymbol{k}_t$, however, must be carried out in the local element coordinate system.

4. ELASTICA

First consider the beam without shear deformation, the Bernoulli-Euler beam, to check the accuracy and convergence of the solutions of Eq. (6). As is clear from Eq. (15), the tangent stiffness matrix is non-symmetric. In order to examine the effect of non-symmetry, consider the Euler buckling of a straight column subjected to the compressive force P. The fundamental solution from Eq. (6) is that the column remains straight; i. e.

$$(u_2-u_1)/l = P/EA \cdots\cdots (19)$$

Substitution of Eq. (19) into the tangent stiffness equation (13) yields

$$\Delta\boldsymbol{f} = [\boldsymbol{k}_{BE}+\boldsymbol{k}_G+O(P/EA)]\Delta\boldsymbol{d} \cdots\cdots (20)$$

from which the buckling load can be obtained as its eigenvalue and where $\boldsymbol{k}_{BE}$ is the linear stiffness matrix of the Bernoulli-Euler beam, and $\boldsymbol{k}_G$ the geometric stiffness. $\boldsymbol{k}_{BE}$ and $\boldsymbol{k}_G$ correspond to $\boldsymbol{k}_L$ and $\boldsymbol{k}_{NL}$ in Eq. (11) with no shear; i. e. $\alpha=0$, respectively. Since P/EA is the axial strain of a column, the third term in the blacket of Eq. (20) can be negligible compared with the other two terms, as long as the small strain assumption holds. Therefore the tangent stiffness matrix is almost symmetric and has the ordinary form of the sum of linear and geometric stiffness matrices. Judging from this result, we can expect that the non-symmetry effect is as the same order as the strain components.

The numerical solutions of the discretized equation are then examined by the simple problem of an

elastica, the analytic solutions of which are expressed by the elliptic integrals[11),12)]. The absolute errors of the lateral displacement are shown for a certain number of elements in Fig. 2. In the numerical calculation, the slenderness ratio is set 10^6, because the elastica is the inextensible rod and thus can be approximated by the beam with very large slenderness ratio. When the geometric stiffness matrix is included, the solutions are closer to the analytic ones than those without it for a certain number of elements. Furthermore, the convergence is much faster when the geometric stiffness is included, but the results without it also converge to the same exact solutions.

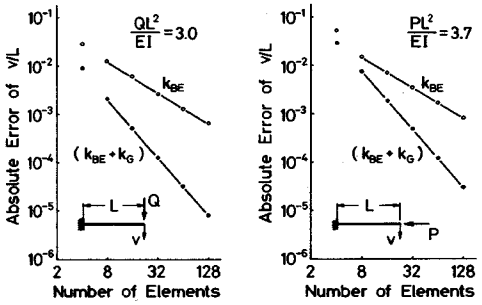

Fig. 2 Convergence of Discretized Solutions for Elastica.

5. CORRESPONDING DIFFERENTIAL EQUATION AND GEOMETRIC STIFFNESS MATRIX

Since the Bernoulli-Euler beam does not always need the geometric stiffness matrix, we here derive the differential equation which corresponds to the discretized equation (6) without the geometric stiffness, k_{tNL}. To this end, the technique to check the consistency of the finite difference equations[13)] is used. The same technique has been used to show the validity of the analysis of curved beams by the assemblage of straight beam elements[14)]. Let u, v and λ denote the translational and rotational displacement components, and let N, V and M denote the axial and shear resultant forces and the bending moment. Quite cumbersome manipulation on Eq. (6) leads to the differential equations as

$$\left.\begin{aligned} &\{N\cos\lambda - V\sin\lambda\}'=0, \quad \{N\sin\lambda + V\cos\lambda\}'=0, \quad M'+V=0 \\ &u'=(1+N/EA)\cos\lambda-(V/GKA)\sin\lambda-1 \\ &v'=(1+N/EA)\sin\lambda+(V/GKA)\cos\lambda, \quad \lambda'=M/EI \end{aligned}\right\} \cdots\cdots (21)$$

where a prime stands for the differentiation with respect to x. In the Appendix, the various approximated theories of the Timoshenko beam obtained in Ref. 10) are enumerated. The equations above are identical with the "small strain" approximation of the 1st order theory ; (C) in the Appendix. Figs. 3 and 4 show the convergence of the discretized solutions with shear effect for the same problems examined for the Bernoulli-Euler beam in the preceding section. The dashed lines indicate the change of such solutions without the geometric stiffness matrix. These lines seem to converge to the level shown by the horizontal lines with a letter "C" at the right hand sides of figures. This horizontal lines with "C" show the numerical-integral solutions of the differential equation (21) by a shooting method[15)]. All other horizontal lines indicate the similar solutions of the differential equations in the Appendix specified by the affixed letters from "A" to "F".

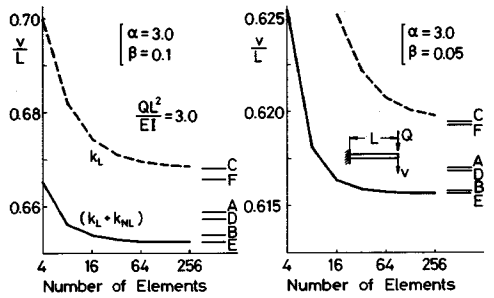

Fig. 3 Convergence of Discretized Solutions of Timoshenko Beam (Shear).

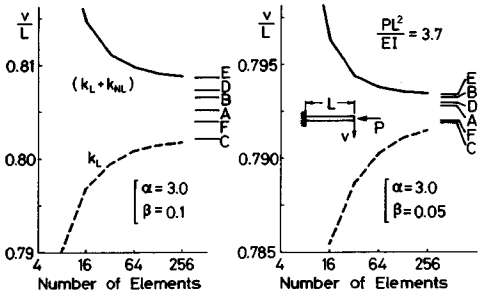

Fig. 4 Convergence of Discretized Solutions of Timoshenko Beam (Compression).

In the same figures, the change of the discretized solutions with the geometric stiffness matrix is also shown by the solid lines. Unlike the Bernoulli-Euler beam, the solutions with or without the geometric stiffness converge to the different answers. The solutions to which the solid lines seem to converge are the ones by the theory (E), the "small extension" approximation of the 2nd order theory. Although the differential equation which corresponds to the stiffness equation with the geometric stiffness is not derived because of its cumbersome procedure, these numerical check of the convergence may support that the discretized solutions are the approximated ones of theory (E).

In the Appendix, the buckling formulae of a column are also summarized for each one of theories. Since the buckling load obtained from the theory (C) is the same as the Euler buckling load, the theory (C) does not completely take the effect of shear deformation into account. On the other hand, the theory (E) predicts the same critical load as that obtained by Engesser's formula. Judging from the difference of these predicted buckling loads by both theories, we must conclude that the geometric stiffness matrix cannot be neglected in the calculation of the Timoshenko beam. If the shear deformation is neglected, these theories (C) and (E) are identical. Therefore the geometric stiffness matrix is not always necessary for the Bernoulli-Euler beam.

6. STABILITY OF SIMPLE STRUCTURES

We here show the results of the typical stability problems as illustrative examples. Since the available solutions to be compared are mainly for the slender beams, the shear effect is neglected in the results of this section. Fig. 5 shows the load-displacement relation of a non-symmetric circular deep arch[16], which has been also calculated in Ref. 2) and recently in Ref. 17). In the process of the Newton-Raphson method, an elimination method is used to solve the simultaneous equation. After the forward elimination, if there exists at least one negative element among the diagonal elements of the tangent stiffness matrix, one of the eigenvalues becomes negative, and thus the tangent stiffness is no longer positive definite. The number of these negative diagonal elements of the matrix is the same as that of the negative eigenvalues. Therefore, chasing the change of the number of these negative elements, we can find the bifurcation points along that equilibrium path without consuming time to carry out the eigenvalue analysis.

Although the bifurcation points are not searched systematically in these numerical examples, numbers attached in the following figures indicate the number of these negative elements. As has been pointed out in Ref. 17), no bifurcation point can be found in the equilibrium path shown in this figure. The equilibrium paths for more slender arches, for example, with $R/\sqrt{I/A}$ larger than 700, are the same as that in Fig. 5, but the number of negative eigenvalues can not be determined stably due to the numerical errors, because we did not do any preprocessing of the tangent stiffness matrix, such as normalization.

On the other hand, the symmetric circular arch in Fig. 6 is relatively deep so that the non-symmetric

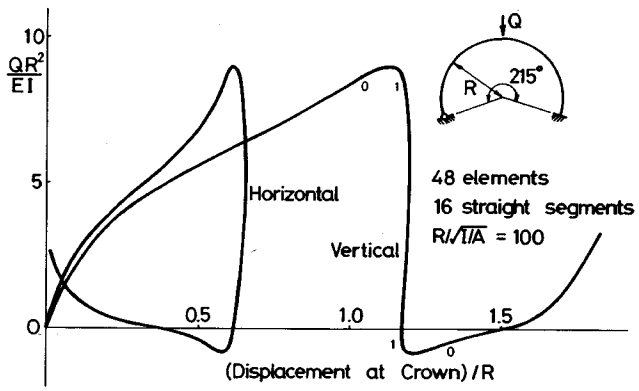

Fig. 5 Large Deformation of a Circular Hinged-Clamped Arch.

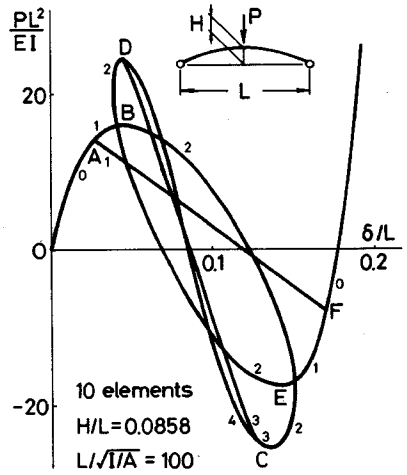

Fig. 6 Non-Symmetric Bifurcation of a Shallow Circular Arch; δ is the vertical displacement of crown.

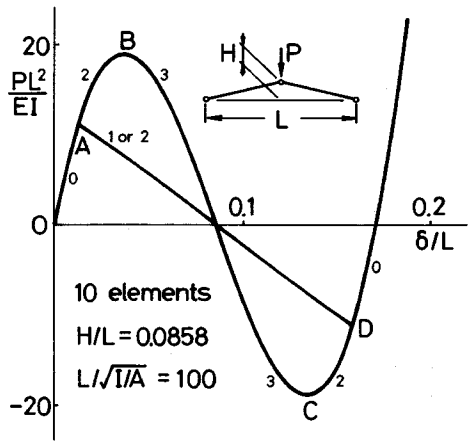

Fig. 7 Non-Symmetric Bifurcation of a Three-Hinged-Arch-like Frame; δ is the vertical displacement of the loaded point.

buckling occurs at point A before the maximum load is achieved at B[18]. The fundamental path from C to D may be the curved one with the symmetric deformation. The steeper path from C to D corresponds to the non-symmetric deformation with some rotation at the crown. There exists short path with three negative elements between bifurcation point and lower extreme point near C. The structure is stable along the paths before A and after F.

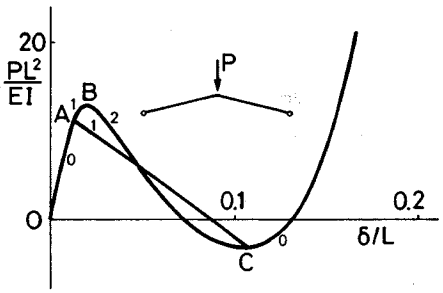

Fig. 8 Non-Symmetric Bifurcation of a Two-Hinged Frame.

Fig. 7 shows the behavior of a "pin-jointed frame", the profile of which is similar to the arch in Fig. 6. The hinge at the loaded point is inserted by the technique described in Ref. 19). Since the component members are relatively slender, there exists one bifurcation point before this structure shows the snap-through phenomenon at B, although a "truss" with the same geometry does not show such a bifurcation because of its rather small rise H without bending freedom[20]. At the bifurcation point, the axial forces of both members reach the level of the Euler buckling load of a hinged-hinged column. The configuration along this bifurcated path is sensitive to the trial solutions assumed to search the possible equilibrium state after the bifurcation. If both members are currently bended either symmetrically or antisymmetrically, the bifurcated configurations are also either symmetric or antisymmetric with one negative diagonal element in the tangent stiffness matrix. If one of the members is kept straight and another is bended, the configuration is the same as this initial trial solution, and one of the members remains straight with two negative elements in the stiffness. However, independently of these assumed trial solutions, the bifurcated paths are identical on this figure. As the member becomes stocky, this bifurcation point A relatively approaches toward the peak point B, because the Euler buckling load is also becoming larger. For such stocky members, for example, $L/\sqrt{I/A}$ smaller than 60, this structure can be really called a truss; i. e. the Euler buckling load becomes larger than the snap-through load. Hence the bifurcation point eventually vanishes, and only the snap-through instability occurs.

Finally if the members in Fig. 7 are rigidly connected at the crest, the load-deflection curve becomes different as is in Fig. 8. Before the maximum point is achieved, the bifurcation also occurs. The related study on number of negative elements has been reported[18),21)].

7. CONCLUDING REMARKS

The stiffness equation, not the "tangent" stiffness, for plane frames is derived by the physical interpretation of the polar decomposition theorem. The basic concept lies in the same consideration as the approximation of curved beams by the assemblage of straight beams, because to analyze the equilibrium in the deformed configuration is substantially the problem of the curved beam. A method to check the consistency of finite difference equation has been employed to obtain the corresponding differential equation to the stiffness equation without the geometric stiffness. The other differential equations are also enumerated, and the convergence of the solutions of discretized equation with the geometric stiffness to those of the differential equations is demonstrated numerically. Although the geometric stiffness matrix is not always necessary to solve the Bernoulli-Euler beam, it can never be neglected to solve the Timoshenko beam which corresponds to the differential equation for the "small extension" approximation of the "2nd" order theory.

It must be noted that the solution of this stiffness equation does not satisfy the real equilibrium condition even when the infinite number of elements are taken. However the difference between the approximate solutions and the real equilibrium solutions is the same order as strains. This difference stems from the approximation of the moment equilibrium with shear force as shown in Appendix. The nonlinearity in this moment equilibrium can never be taken into account by the present formulation, as long as the linearized conventional stiffness matrix is used. The solutions of typical stability problems show the ability of this discretized equation. The bifurcation phenomena and the snap-through-type buckling can be searched by chasing the number of the negative diagonal elements even in the non-symmetric tangent stiffness matrix.

A computer program used here is developed for a micro-computer. The arc length method[18] is employed to estimate the post-buckling behavior properly, and the skyline technique[22] is adopted to use memory effectively.

APPENDIX. TIMOSHENKO BEAM THEORIES

We here simply enumerate two basic theories and their approximations of the Timoshenko beam formulated in Ref. 10). Since the boundary conditions for all theories below are completely the same as those in Ref. 10), only the differential equations are shown. The following nine theories are also summarized in Table 1. In this table, "No" in the last item, "Strict Equilibrium", indicates that the theory is not a physical one but an approximated one, and that the equilibrium is not rigorously satisfied because of such approximations.

(A) The first order theory, extensible

Table 1 Comparison of Timoshenko Beam Theories.

Constitutive Equations	$N = EA\,\varepsilon$, $V = GA\,\gamma$			$M = EI\,\kappa$, $V = (GA + N)\,\gamma$					
Shear Effect	included			neglected			included		
Theory	A	B	C	G	I	H	D	E	F
Buckling Formula	Modified + Shortening	Modified	Euler	Euler + Shortening	Euler		New	Engesser	Euler
Local Stiffness	-	-	$\mathbf{k}_L$	-	(*) $\mathbf{k}_{BE}$ or $\mathbf{k}_{BE}+\mathbf{k}_G$		-	$\mathbf{k}_L+\mathbf{k}_{NL}$	-
Strict Equilibrium	Yes	No		Yes		No	Yes	No	

(*) Inextensible beam (elastica) can be analyzed with very large slenderness ratio.

The first order theory assumes the constitutive relations by

$$N=EA\varepsilon,\quad M=EI\varkappa,\quad V=GA\gamma \cdots\cdots (A\cdot1)$$

where ε is the extension of a beam; $\varkappa$ the curvature; γ the shear deformation. Then the governing differential equations are written as follows:

$$\left.\begin{aligned} &\{N\cos\lambda-V\sin\lambda\}'+p=0,\quad \{N\sin\lambda+V\cos\lambda\}'+q=0\\ &M'+V(1+N/EA)-N(V/GA)=0,\quad u'=(1+N/EA)\cos\lambda-V/GA\sin\lambda-1\\ &v'=(1+N/EA)\sin\lambda+V/GA\cos\lambda,\quad \lambda'=M/EI \end{aligned}\right\} \cdots\cdots (A\cdot2)$$

where p and q are the x- and y-components of the distributed load per unit axial length. The buckling formula for a hinged-hinged column predicted by this theory is the modified formula with the shortening effect, and is expressed as

$$\psi\equiv P_{cr}L^2/EI=\{1-\sqrt{1-4\pi^2\beta^2(1-\alpha)}\}/\{2\beta^2(1-\alpha)\} \cdots\cdots (A\cdot3)$$

(B) Small extension approximation of the first order theory

If the axial extension effect in the equilibrium of moment is neglected as a small quantity, the third equation of Eq. (A·2) must be replaced by

$$M'+V-N(V/GA)=0 \cdots\cdots (A\cdot4)$$

The buckling formula is then identical with the modified formula as

$$\psi=\{\sqrt{1+4\pi^2\alpha\beta^2}-1\}/(2\alpha\beta^2) \cdots\cdots (A\cdot5)$$

(C) Small strain approximation of the first order theory

If the small strain applies in this moment equilibrium, Eq. (A·4) must be further approximated as

$$M'+V=0 \cdots\cdots (A\cdot6)$$

and therefore Eq. (21) is obtained. The bucklng load is finally identical with the Euler load which does not include any effect of shear deformation; i. e.

$$\psi=\pi^2 \cdots\cdots (A\cdot7)$$

Note, however, that the shear effect is still taken into account in the fourth and fifth equations of the governing equations, which are the kinematic relations.

(D) The Second order theory, extensible

The second order theory is based on a different constitutive relation for shear force, which is expressed by

$$V=(GA+N)\gamma \cdots\cdots (A\cdot8)$$

Other two relations in Eq. (A·1) hold. Then the governing equations different from Eq. (A·2) are the third, fourth and fifth equations expressed by

$$\left.\begin{aligned} &M'+V(1+N/EA)-N(V/GA)/\underline{(1+N/GA)}=0\\ &u'=(1+N/EA)\cos\lambda-V/GA\sin\lambda/\underline{(1+N/GA)}-1\\ &v'=(1+N/EA)\sin\lambda+V/GA\cos\lambda/\underline{(1+N/GA)} \end{aligned}\right\} \cdots\cdots (A\cdot9)$$

where the underlined terms do not appear in the first order theory. The buckling load is expressed by the following implicit equation:

$$\pi^2=\psi/(1-\alpha\beta^2\psi)-\beta^2\psi^2 \cdots\cdots (A\cdot10)$$

(E) Small extension approximation of the second order theory

The similar approximation in (B) is applied to obtain the moment equilibrium as

$$M'+V-N(V/GA)/(1+N/GA)=0 \cdots\cdots (A\cdot11)$$

This approximated theory predicts the same buckling load as Engesser's formula; i. e.

$$\psi=\pi^2/(1+\alpha\beta^2\pi^2) \cdots\cdots (A\cdot12)$$

(F) Small strain approximation of the second order theory

Eq. (A·11) is further approximated by the small strain assumption to get the same equation as Eq. (A·6). The obtained buckling formula is again the same as the Eular load, Eq. (A·7).

(G) Bernoulli-Euler beam, extensible

If the shear effect is neglected, both the first and second theories result in the same theory, the

extensible Bernoulli-Euler beam theory. The governing equations are the same as Eq. (A·2) except the following three equations :

$$M'+V(1+N/EA)=0, \quad u'=(1+N/EA)\cos\lambda-1, \quad v'=(1+N/EA)\sin\lambda \cdots\cdots (A\cdot13)$$

The buckling formula includes the shortening effect prior to the buckling, and is expressed as

$$\psi=\{1-\sqrt{1-4\pi^2\beta^2}\}/(2\beta^2) \cdots\cdots (A\cdot14)$$

(H) Small extension (strain) approximation of the Bernoulli-Euler beam

If the extension is neglected in the equlibrium equation of moment as a small quantity, it becomes the same as Eq. (A·6), and the buckling load is given by the Euler load, Eq. (A·7).

(I) Inextensible Bernoulli-Euler beam (elastica)

If the beam is so slender that the extension is negligibly small compared with the bending strain, Eq. (A·13) must be replaced by the following equations.

$$M'+V=0, \quad u'=\cos\lambda-1, \quad v'=\sin\lambda \cdots\cdots (A\cdot15)$$

The buckling load is identical with the Euler load.

REFERENCES

1) Goto, S., Hane, G. and Tanaka, T. : Tangent stiffness method for large deformation analysis of frame structure, Proc. JSCE, No. 238, pp. 31~42, 1975 (in Japaneses).
2) Yoshida, Y., Masuda, N., Morimoto, T. and Hirosawa, N. : An incremental formulation for computer analysis of space framed structures, Proc. JSCE, No. 300, pp. 21~31, 1980 (in Japanese).
3) Yoshida, Y., Nomura, T. and Masuda, N. : A formulation and solution procedure for post-buckling of thin-walled structures, Comp. Meth. Appl. Mech. Eng., Vol. 32, pp. 285~309, 1982.
4) Maeda, Y. and Hayashi, M. : Finite displacement analysis of space framed structures, Proc. JSCE, No. 253, pp. 13~27, 1976 (in Japanese).
5) Goto, Y., Hasegawa, A. and Nishino, F. : Accuracy of finite displacement analysis of plane frames, Proc. JSCE, No. 331, pp. 33~44, 1983 (in Japanese).
6) Kondoh, K. and Atluri, S. N. : A simplified finite element method for large deformation, post-buckling analyses of large frame structures, using explicitly derived tangent stiffness matrices, Int. J. Numer. Meth. Eng., Vol. 23, pp. 69~90, 1986.
7) Iura, M. and Hirashima, M. : Geometrically nonlinear theory of naturally curved and twisted rods with finite rotations, Structural Eng./Earthquake Eng., Japan Society of Civil Engineers, Vol. 2, pp. 353 s~363 s, 1985.
8) Malvern, L. E. : Introduction to the Mechanics of a Continuous Medium, Prentice-Hall, Inc., New Jersey, 1969.
9) Hasegawa, A., Iwakuma, T. and Kuranishi, S. : A linearized Timoshenko beam theory in finite displacements, Structural Eng./Earthquake Eng., Japan Society of Civil Engineers, Vol. 2, pp. 321 s~326 s, 1985.
10) Iwakuma, T. and Kuranishi, S. : How much contribution does the shear deformation have in a beam theory?, Structural Eng./Earthquake Eng., Japan Society of Civil Engineers, Vol. 1, pp. 103 s~113 s, 1984.
11) Timoshenko, S. P. and Gere, J. M. : Theory of Elastic Stability, 2nd. ed., McGraw-Hill Kogakusha Ltd., Tokyo, 1961.
12) Bisshopp, K. E. and Drucker, D. C. : Large deflection of cantilever beams, Q. Appl. Math., Vol. 3, pp. 272~275, 1945.
13) Yamamoto, Y. and Yamada, Z. : Errors on the Matrix Structural Analysis, Series of Computational Structural Engineering, Vol. II-5-B, Baifu-Kan, Tokyo, 1972 (in Japanese).
14) Yoda, T. : Validity and accuracy of straight beam element approximation for the analysis of curved beams, Theoretical and Applied Mechanics, Proc. 33rd Japan Nat. Cong. for Appl. Mech., pp. 171~178, Univ. Tokyo Press, 1985.
15) Roberts, S. M. and Shipman, J. S. : Two-Point Boundary Value Problems : Shooting Methods, American Elsevier Pub. Co., Inc., New York, 1972.
16) DaDeppo, D. A. and Schmidt, R. : Instability of clamped-hinged circular arches subjected to a point load, J. Appl. Mech., Vol. 42, pp. 894~896, 1975.
17) Chaisomphob, T., Nishino, F., Hasegawa, A. and Aly Gamal Aly A.-S. : An elastic finite displacement analysis of plane beams with and without shear deformation, Structural Eng./Earthquake Eng., Japan Society of Civil Engineers, Vol. 3, pp. 157 s~165 s, 1986.
18) Hosono, T. : Analysis of elastic buckling problem by arc length method (Part 2), Trans. Architectural Institute of Japan, No. 243, pp. 21~31, 1976 (in Japanese).
19) Hasegawa, A., Iwakuma, T., Liyanage, K. and Nishino, F. : A consistent formulation of trusses and non-warping beams in linearized finite displacements, Structural Eng./Earthquake Eng., Japan Society of Civil Engineers, Vol. 3, pp. 477 s~480 s, 1986.
20) Pecknold, D. A., Ghaboussi, J. and Healey, T. J. : Snap-through and bifurcation in a simple structure, J. Eng. Mech.,

American Society of Civil Engineers, Vol. 111, pp. 909~922, 1985.

21) See, T. and McConnel, R. E. : Large displacement elastic buckling of space structures, J. Struct. Eng., American Society of Civil Engineers, Vol. 112, pp. 1052~1069, 1986.

22) Elwi, A. E. and Murray, D. W. : Skyline algorithms for multilevel substructure analysis, Int. J. Numer. Meth. Eng., Vol. 21, pp. 465~479, 1985.

(Received June 18 1986)